AD-A141 630 WAVE-LESS FREE-SURFACE PRESSURE DISTRIBUTIONS(U) 1/1
WISCONSIN UNIV-MADISON MATHEMATICS RESEARCH CENTER
J M VANDEN-BROECK ET AL. APR 84 MRC-TSR-2679
UNCLASSIFIED DAAG29-80-C-0041 F/G 20/4 NL

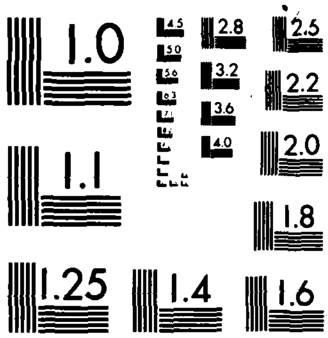

MICROCOPY RESOLUTION TEST CHART
NATIONAL BUREAU OF STANDARDS-1963-A

2

AD-A141 630

MRC Technical Summary Report #2679

WAVE-LESS FREE-SURFACE PRESSURE DISTRIBUTIONS

J.-M. Vanden-Broeck and E. O. Tuck

Mathematics Research Center
University of Wisconsin—Madison
610 Walnut Street
Madison, Wisconsin 53705

April 1984

(Received April 2, 1984)

Approved for public release
Distribution unlimited

Sponsored by

U. S. Army Research Office
P. O. Box 12211
Research Triangle Park
North Carolina 27709

National Science Foundation
Washington, DC 20550

UNIVERSITY OF WISCONSIN-MADISON
MATHEMATICS RESEARCH CENTER

WAVE-LESS FREE-SURFACE PRESSURE DISTRIBUTIONS

J.-M. Vanden-Broeck* and E. O. Tuck**

Technical Summary Report #2679
April 1984

ABSTRACT

Linear and nonlinear studies are made of two-dimensional free-surface flows under gravity, in which a disturbance is caused to an otherwise-uniform stream by a distribution of pressure over the free surface. In general, such a disturbance creates a system of trailing waves. However, there are special disturbances that do not, and some categories of such disturbances are discussed here. This work has potential applications to design of splash-less ship bows.

AMS (MOS) Subject Classifications: 76B20

Key Words: Bow flow, free surface flows

Work Unit 2 (Physical Mathematics)

*Department of Mathematics and Mathematics Research Center, University of Wisconsin-Madison, Madison, WI 53705
**Applied Mathematics Department, The University of Adelaide, S.A. 5000, Australia

Sponsored by the United States Army under Contract No. DAAG29-80-C-0041 and the National Science Foundation under Grant MCS800-1960. A part of this work was supported by the Australian Research Grants Scheme during a visit of the first author to the University of Adelaide.

SIGNIFICANCE AND EXPLANATION

One of the important problems of modern ship hydrodynamics concerns the flow at the extreme bow. In particular, reduction and, if possible, elimination of the splash, and resulting splash drag is of great interest.

In the present paper linear and nonlinear studies are made of two-dimensional flows, in which an otherwise uniform stream is disturbed by a distribution of pressure over the free surface. It is found that some families of pressure distributions do not generate waves. These wave-less flows generate candidate shapes for splash-less bows.

WAVE-LESS FREE-SURFACE PRESSURE DISTRIBUTIONS

J.-M. Vanden-Broeck* and E. O. Tuck**

1. *Introduction*

One of the important problems of modern ship hydrodynamics concerns the flow at the extreme bow. In particular, prediction and, if possible, elimination of the splash, and resulting splash drag component is of great interest. It appears (c.f. refs [1,2]) that one of the roles of a bulbous bow is to effect just such an elimination (or at least reduction in magnitude) of the splash drag under suitable conditions of speed and loading.

In previous research [3,4] the present authors have considered fundamental questions associated with a two-dimensional model for such bow flows. That work suggested that, for a given bow shape, splash-free solutions may not exist. However, only special (specifically non-bulbous) bow shapes were used in the previous studies. The possibility exists that, by considering suitable *families* of bow shapes, one could identify a special shape having the splash-free property. In the linearised case, such shapes have been considered by Schmidt [5].

*Department of Mathematics and Mathematics Research Center, University of Wisconsin-Madison, Madison, WI 53705

**Applied Mathematics Department, The University of Adelaide, S.A. 5000, Australia

Sponsored by the United States Army under Contract No. DAAG29-80-C-0041 and the National Science Foundation under Grant MCS800-1960. A part of this work was supported by the Australian Research Grants Scheme during a visit of the first author to the University of Adelaide.

In the present article, we approach this problem in an indirect manner. If such a special bow exists, and if one computes the pressure exerted on it by the water, then one can replace the original body by an artificial prescribed pressure distribution over the free-surface. Conversely, if one *starts* with a given free-surface pressure distribution, the streamlines generated will define a candidate bow shape.

The obvious difficulty with this approach is that, in general, such pressure distributions generate a train of waves downstream, and we are (ultimately) looking for flows that are not only splash-free, but also wave-free. However, it is well known (c.f.[6], p.404) that in two dimensions there exist special pressure distributions whose downstream wave amplitude is zero, and our main purpose here is to enumerate and discuss such special cases.

In particular, suppose we consider a family of pressure distributions that vanish for $x > 0$, and tend to a positive constant value as $x \to -\infty$. This pressure will in general correspond to a semi-infinite "stern" profile having finite draft at $x = -\infty$, and producing a train of waves downstream at $x = +\infty$. Within this family there may be one or more special members for which the downstream wave amplitude is zero. Since there are no waves, the radiation condition does not apply to such special solutions, and the flow direction can be reversed, so generating a semi-infinite 'bow' flow. This flow possesses neither a splash nor (*upstream*) waves, and hence is precisely of the type desired.

The above discussion proceeds without any consideration of linearisation. However, few demonstrations have been made of non-linear free-surface flows without downstream waves, and it is not entirely obvious that they exist, although the numerical evidence [7,8] is strong, and the approximate non-linear theory of Tulin [9] can be interpreted as providing indirect analytic confirmation.

Here we first discuss the linearised case in some detail, enumerating some families of wave-less pressure distributions, and computing the corresponding free-surface contour. This contour can then be replaced by a fixed body, but only as an approximation when that body has a small stream-wise slope everywhere, in order that the generating pressure can be small to justify linearisation. Some of the results suggest bulbous character, but of course a true bulb can never be attained with such a restriction on the body's slope. These linear results can be viewed as an inverse re-formulation of the theory of Schmidt [5].

We then solve the non-linear problem by a perturbation procedure, in which the linearised solution is viewed as the first term in an asymptotic expansion with respect to some small parameter ϵ. Thus, ϵ measures either (and both) the body's streamwise slope and the size of the pressure distribution that generates it. In principle, providing we adopt a careful inverse formulation with the velocity potential as *independent* variable, any number of terms in the asymptotic expansion in powers of ϵ can be computed, for continuous pressure distributions. We provide here some 2nd-order numerical results, and higher-order results seem to be not hard to obtain. This is, however, not true if the input pressure possesses step-function discontinuities, because singularities occur whose degree increases with the power of ϵ.

An alternative approach to non-linear free-surface solution is via exact inverse methods, c.f. [10,11]. That is, it is possible to write down a specification for the flow in which all requisite equations (including the non-linear free-surface condition) are satisfied *exactly*. This has not in the past proved a very useful technique because of the unrealistic nature of the streamlines generated. However, the extra freedom obtained by allowing a non-zero free-surface pressure, enables us to get a little closer to practical applicablility. The price paid for this is that we cannot expect the inversely-obtained pressure distributions to be exactly zero anywhere on the free surface. The best we can do is to cause the pressure to be very small over a portion of the streamline that is a candidate for a true "free" surface.

2. *Weak Pressure Distributions*

Suppose that the only disturbance to a uniform stream of unit magnitude in the +x-direction consists of a small departure $P(x)$ from the equilibrium atmospheric value of the free-surface pressure. If $P(x)$ is sufficiently small, and we make the usual assumptions [12] of classical linearised water-wave theory we find (c.f. [13]) that the free-surface elevation is $y = \eta(x)$, where

$$\eta(x) = -P(-\infty) + \int_{-\infty}^{\infty} P'(\xi)K(x-\xi)\, d\xi. \qquad (2.1)$$

The kernel function $K(x)$ is the wave elevation due to a unit-step pressure, namely

$$K(x) = -\frac{1}{\pi}f(x) + \begin{cases} 2\cos x - 1, & x > 0 \\ 0 \quad , & x < 0, \end{cases} \qquad (2.2)$$

where

$$f(x) = \mathrm{Ci}(|x|)\sin x - \mathrm{si}(|x|)\cos x \,\mathrm{sgn}\, x \qquad (2.3)$$

is the odd auxiliary function ([14], p.232) of the sine and cosine integrals.

Note that we have non-dimensionalised so that not only is the free stream of unit magnitude, but the acceleration of gravity and the density are both also of unit magnitude. In effect, we have chosen a length scale of magnitude U^2/g, and a pressure scale of magnitude ρU^2, where U, g and ρ are the actual values of these quantities. Since the wavelength of linearised waves is $2\pi U^2/g$, this means that in the present non-dimensional framework, their length is 2π, as is clear from the term in cos x in (2.2).

In fact, since f(x) tends to zero at infinity, as $x \to +\infty$ we have

$$\eta(x) \to -P(-\infty) + \int_{-\infty}^{x} P'(\xi)[2\cos(x-\xi)-1]d\xi$$

$$\to -P(+\infty) + 2\int_{-\infty}^{\infty} P'(\xi)\cos(x-\xi)d\xi. \qquad (2.4)$$

However, from now on we assume (without loss of generality) that $P(+\infty) = 0$, i.e. that the pressure is allowed to return to atmospheric far *downstream*, and hence that the mean free-surface level downstream is defined to be the level at which $y = 0$. In that case, (2.4) reduces to

$$\eta(x) \to [2\int_{-\infty}^{\infty} P'(\xi)\cos\xi\, d\xi]\cos x + [2\int_{-\infty}^{\infty} P'(\xi)\sin\xi\, d\xi]\sin x \qquad (2.5)$$

i.e. there is a wave at $x = +\infty$, whose magnitude and phase are determined by the pressure distribution P(x). This wave disappears if and only if

$$\int_{-\infty}^{\infty} P'(x)\cos x\, dx = 0 \qquad (2.6)$$

and

$$\int_{-\infty}^{\infty} P'(x)\sin x\, dx = 0. \qquad (2.7)$$

Any pressure distibrution P(x) satisfying (2.6) and (2.7) will be described as "wave-less".

For example, suppose $P(x)$ is step-wise constant, i.e.

$$P(x) = P_j = \text{constant}, \quad x_{j-1} < x < x_j \tag{2.8}$$

for some set of points x_j, $j=0,1,2,\ldots,N$, where we may take $x_0 = -\infty$ and $x_N = 0$. Then the pressure gradient is a collection of Dirac δ-functions, i.e.

$$P'(x) = \sum_{j=1}^{N} (P_{j+1}-P_j)\delta(x-x_j) \tag{2.9}$$

where $P_{N+1} = 0$. Now (2.6) and (2.7) require

$$\sum_{j=1}^{N} (P_{j+1}- P_j)\cos x_j = \sum_{j=1}^{N} (P_{j+1} - P_j)\sin x_j = 0. \tag{2.10}$$

We can fix one of the constants P_j, say P_1; there are then (2N-2) free parameters P_2, $P_3,\ldots,P_N$, and $x_1,x_2,\ldots,x_{N-1}$, and just two equations restricting them. Clearly there is no wave-less pressure if $N = 1$. This simply confirms that a (single) step-function pressure always generates a trailing wave of non-zero amplitude.

If $N = 2$, there are as many equations as unknowns and a wave-less pressure is possible. The specific form taken by (2.10) is

$$(P_2-P_1)\cos x_1 - P_2 = (P_2-P_1)\sin x_1 = 0 \tag{2.11}$$

Thus, $x_1 = -\pi, -2\pi, -3\pi,\ldots$, so that the step length must be an integer multiple of π. If that integer is *odd*, then $P_1 = 0$ and $P_2 = P_1/2$, i.e. the pressure $P(x)$ consists of a jump at $x = x_1$ to *exactly half* of its (non-zero) upstream value, followed by a jump to zero at the origin. In practice, we are mainly interested in the shortest step, with $x_1 = -\pi$, which corresponds to a Froude number (based on the step length) of $\pi^{-1/2} = .564$.

On the other hand, the solutions with $x_1 = -2\pi$, -4π, -6π,... must have $P_1 = 0$, i.e. correspond to a pressure distribution that vanishes outside the finite segment $x_1 < x < 0$ and is constant within that segment. The existence of such simple finite wave-less pressures is well known; for example, the most important case $x_1 = -2\pi$, with a Froude number of .399, was discussed by Lamb [6] and used by Schwartz [7].

The absence of waves in this case is easy to understand intuitively, since there is exactly one wavelength (2π) between beginning and end of the pressure distribution. Since these ends generate exactly equal and opposite waves, destructive interference is possible. In fact, a similar argument also explains the semi-infinite case $x_1 = -\pi$, where the step length is exactly half a wavelength. Now, in view of the fact that the pressure steps down by a factor of 1/2 at both ends, the waves produced by the ends are exactly equal in magnitude and sign, but now are shifted by a half-wavelength, so that again destructive interference occurs.

In summary, pressure distributions consisting of just two distinct steps can generate wave-less free surfaces, providing the distance between the steps is an integer multiple of the half-wavelength π. The "shortest" such wave-less pressure has a step-length of π, i.e. one half-wavelength, and corresponds to a semi-infinite pressure distribution with constant arbitrary upstream pressure, and a step to exactly half the upstream pressure. The case where the step length is 2π, i.e. a full wavelength, corresponds to zero upstream pressure, and constant arbitrary pressure on the step.

The actual free-surface shape generated by these two pressures is illustrated in Figures 2.1 and 2.2 respectively. In the general case where the pressure is given by (2.8), the free-surface elevation is given by (2.1) as

$$\eta(x) = -P_1 + \sum_{j=1}^{N} (P_{j+1} - P_j) K(x - x_j) \tag{2.12}$$

Since the basic kernel function K is easily computed, this provides a rapid method for evaluating linearised solutions, not only for the present case where P(x) is *exactly* a set of N *steps, with N small, but also for* quite general P(x), as a numerical procedure in which (2.8) is an approximation for large N. Note, however, that wherever P(x) possesses a finite jump discontinuity, $\eta(x)$ is finite but its derivative, the free-surface slope $\eta'(x)$ is infinite. Specifically, if P(x) jumps by ΔP at x = 0, then near x = 0 we have

$$\eta(x) = \eta(0) - \frac{\Delta P}{\pi} x \log|x| + O(x) \tag{2.13}$$

Figures 2.1 and 2.2 show this phenomenon as locally-vertical free surfaces at the points where the pressure jumps.

If we now turn to the case N = 3, since there are now two more parameters than equations, we may expect to obtain a 2-parameter continuous family of wave-less solutions. Equations (2.10) now state

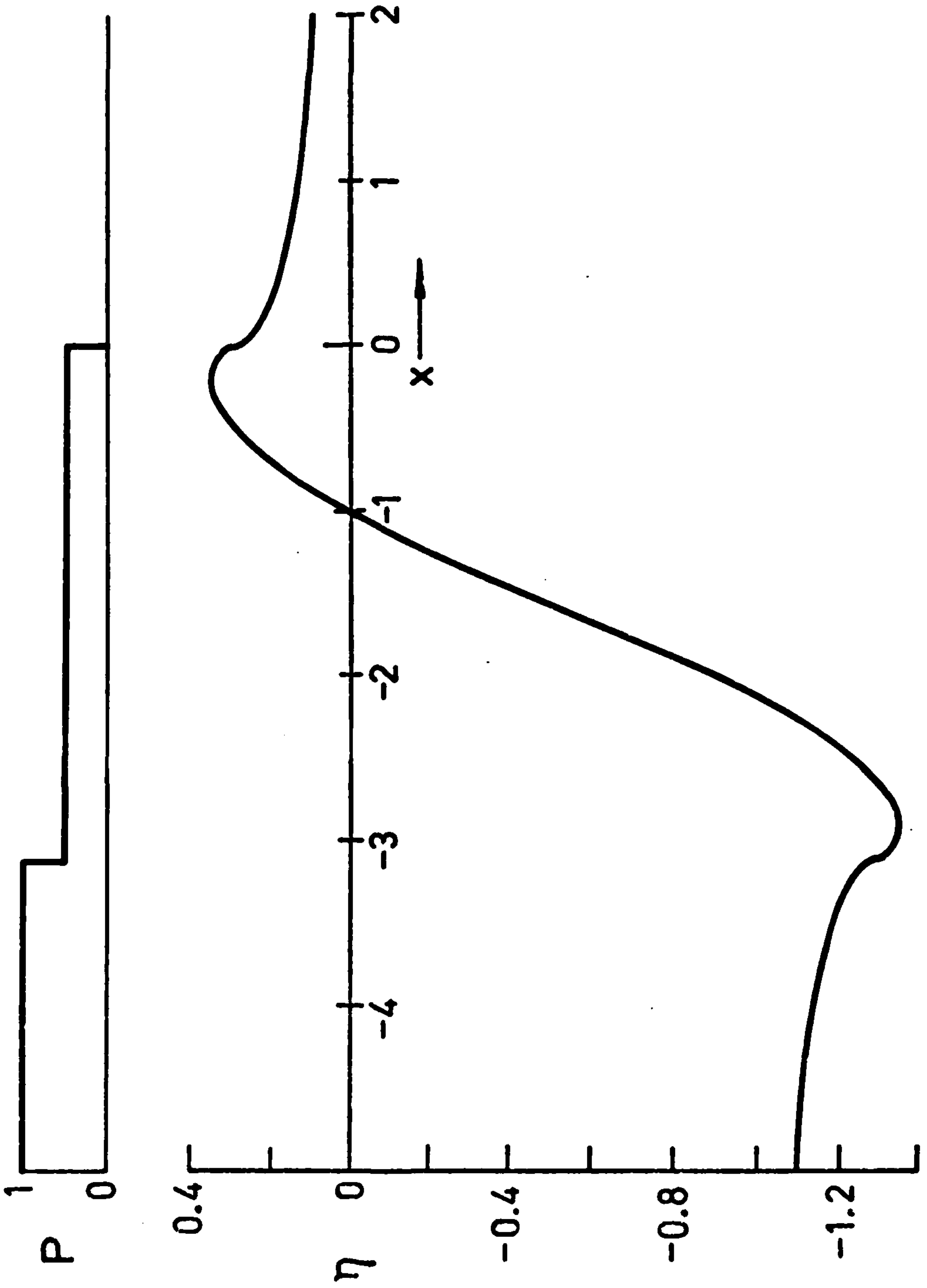

Fig. 2.1

Linearized free surface $\eta(x)$ generated by a wave-less pressure $P(x)$ that jumps from 1 to ½ at $x = -\pi$, then from ½ to 0 at $x = 0$.

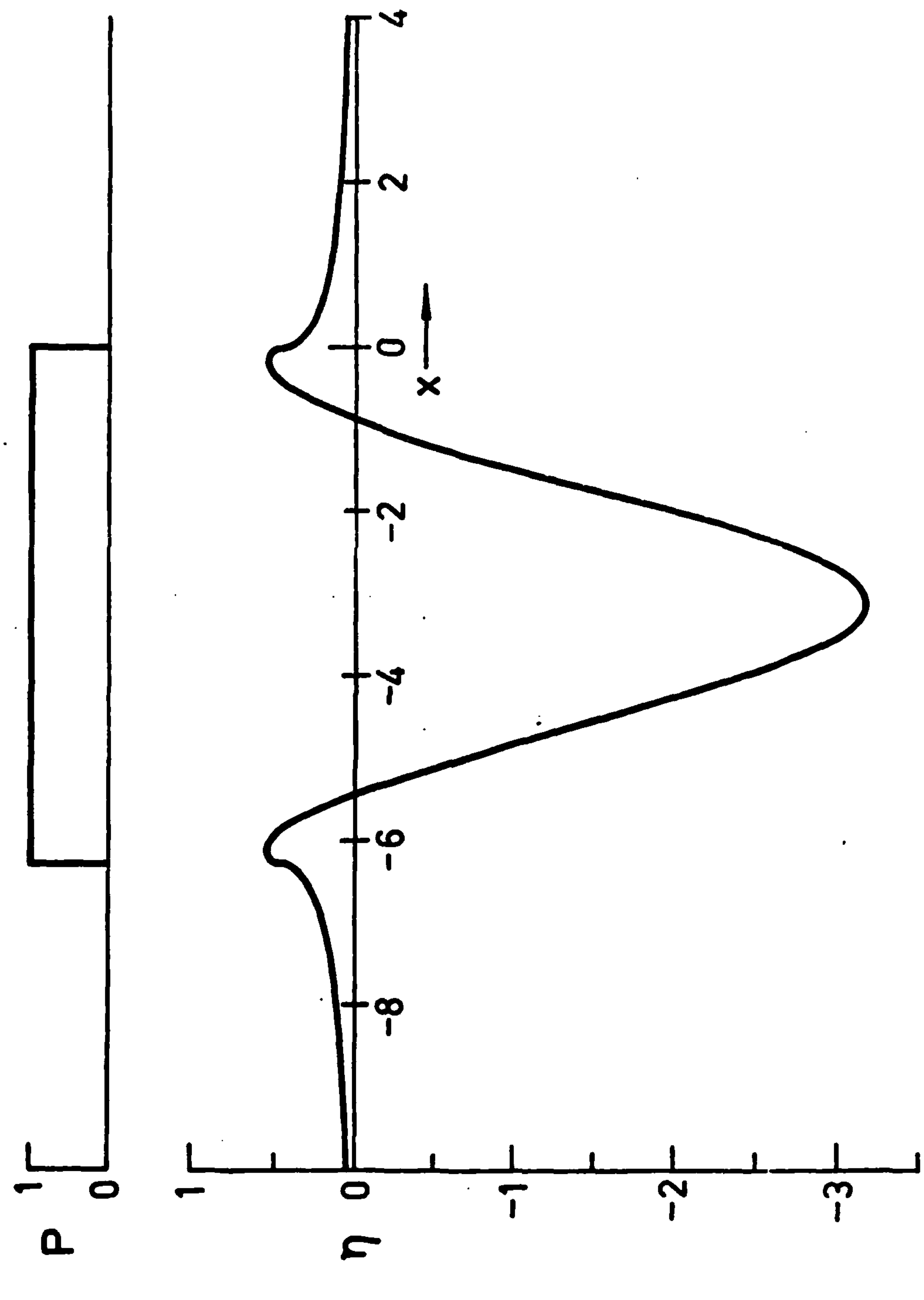

Fig. 2.2

Linearized free surface $\eta(x)$ generated by a wave-less step pressure $P(x) = 1$ for $-2\pi < x < 0$, with $P = 0$ otherwise.

$$(P_2-P_1)\cos x_1 + (P_3-P_2)\cos x_2 - P_3 = 0$$

and

$$(P_2-P_1)\sin x_1 + (P_3-P_2)\sin x_2 = 0 \qquad (2.14)$$

which may be 'solved' for any two of P_1, P_2, P_3, given the third, and the step locations x_1, x_2. This solution may be expressed in the form

$$P_1:P_2:P_3 = s+s_1-s_2:s+s_1:s \qquad (2.15)$$

where $s=\sin(x_2-x_1)$, $s_1=\sin(x_1)$ and $s_2=\sin(x_2)$.

The most useful examples with $N = 3$ are those with $-\pi < x_1 < 0$, since a step length less than π was not achievable for $N = 2$. Figure 2.3 shows (solid curve) a typical example in this category, namely that for $x_1 = -1$, $x_2 = -1/2$. The pressure steps are in the ratios $P_1:P_2:P_3=1:-3.08:4.08$ in this example. If we keep $x_1 = -1$, and vary x_2 in the range $-1 < x_2 < 0$, the free-surface shape does not change very much.

It is interesting to consider the effect of making x_1 even closer to zero. Then we find that (with P_1 normalised to unity) P_2 becomes large and negative, while P_3 becomes large and positive, comparable with $-P_2$. This behaviour corresponds to a combination of a step function and a *dipole in pressure*, i.e. to

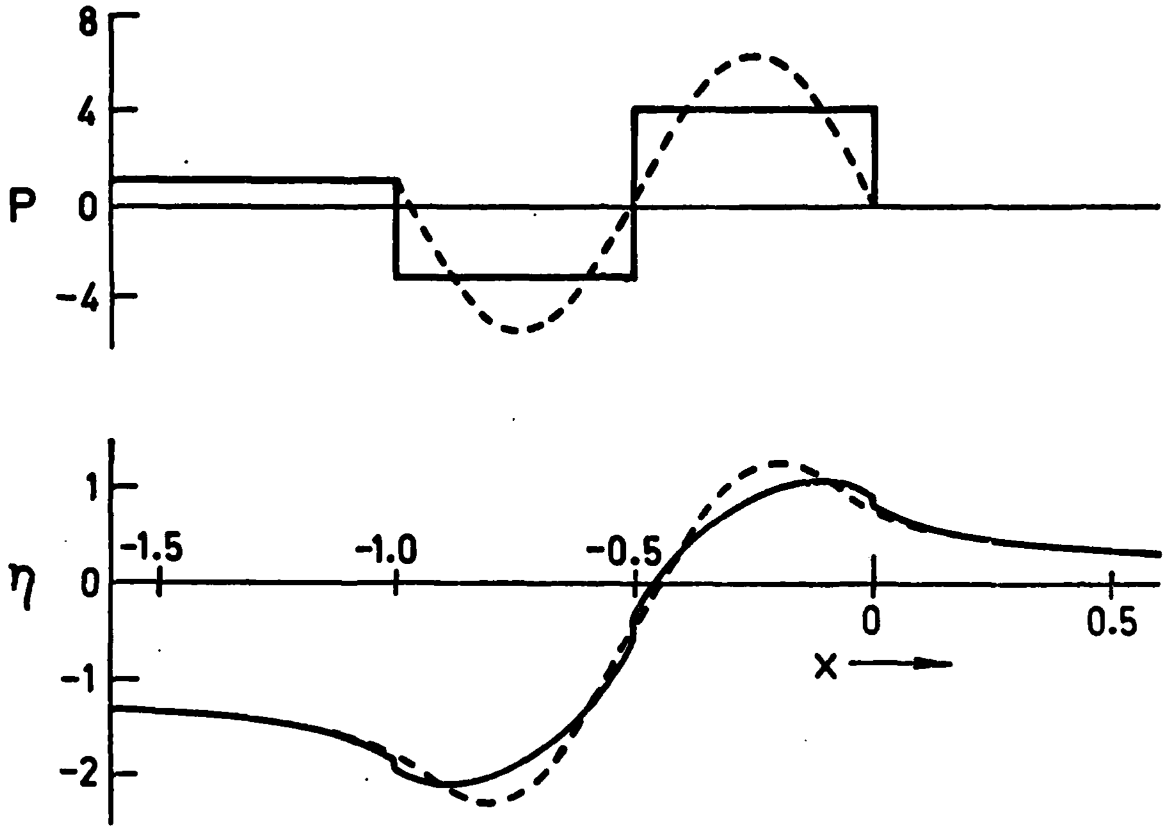

Fig. 2.3

Linearized free surface $\eta(x)$ generated by wave-less pressures $P(x)$ that vary only in $-1 < x < 0$. The solid curve has 3 steps in pressure, the dashed curve has a continuous sinusoidally-varying pressure.

$$P(x) = 1-H(x) - \delta'(x) \tag{2.16}$$

where $H(x)$ is the unit step function. Thus, from (2.1), we have

$$\begin{aligned} \eta(x) &= -1 - K(x) - K''(x) && (2.17) \\ &\to -1 -(2\cos x-1) - (-2\cos x) \\ &\to 0. && \text{as } x \to +\infty \end{aligned}$$

Of course, this limiting solution is very singular at the origin, and for example the free-surface elevation becomes unbounded like $1/x$, but it indicates the possibility of wave-less pressure distributions whose domain of variation is of vanishingly-small length.

The logarithmic singularity (2.13) in the free-surface slope caused by jumps in pressure is barely acceptable in the linearized theory, and becomes (as we shall see) quite unacceptable if the analysis is extended to include non-linearity. It is therefore desirable to consider families of *continuous* pressure distributions. The simplest such example is a linear "pressure ramp"

$$P(x) = \begin{cases} P_1 & , \quad -\infty < x < x_1, \\ P_1 x/x_1 & , \quad x_1 < x < 0 \\ 0 & \quad x > 0 \end{cases} , \tag{2.18}$$

which ~~satisfies~~(2.7) if $x_1 = -2\pi, -4\pi, -6\pi, \ldots\ldots$ Figure 2.4 shows the free-surface shape at $x_1 = -2\pi$. This curve was in fact computed using (2.12) with $N = 40$, which gives 3-4 figure accuracy.

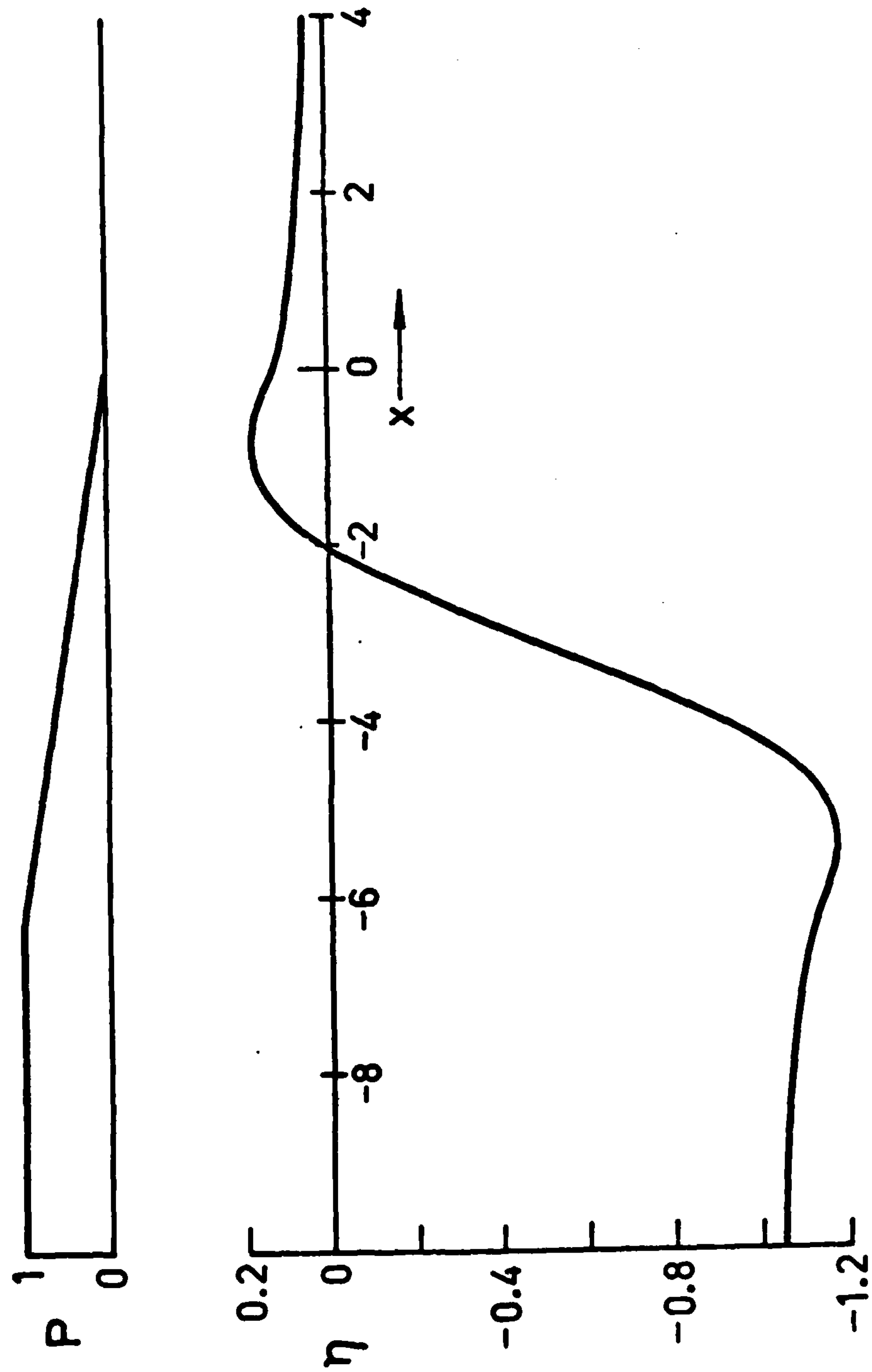

Fig. 2.4

Linearized free surface $\eta(x)$ generated by a continuous wave-less pressure $P(x)$ in the form of a linear ramp over $-2\pi < x < 0$.

A useful one-parameter family of continuous pressures is given by

$$P(x) = \begin{cases} P_1 & -\infty < x < x_1 \\ P_1 \dfrac{x}{x_1} + P_2 \sin \dfrac{2\pi x}{x_1}, & x_1 < x < 0 \\ 0 \quad , & x > 0 \end{cases}$$

which reduces to (2.18) if $P_2 = 0$, but is wave-less for *all* $x_1 < 0$ if

$$\frac{2\pi P_2}{P_1} = \left[\frac{2\pi}{x_1}\right]^2 - 1 \qquad (2.19)$$

Figure 2.3 shows (dashed curve) results at $x_1 = -1$. The solid and dashed curves of this figure contrast discontinuous and continuous wave-less pressures for the same value of x_1, and clearly the smoother pressure gives a smoother but otherwise quite similar free surface.

If one demands an even greater degree of smoothness, then for example

$$P(x) = \begin{cases} P_1 & , \quad -\infty < x < x_1 \\ P_1 \sin^2 \left[\dfrac{\pi x}{2 x_1}\right] & , \quad x_1 < x < 0 \\ 0 & , \quad x > 0 \end{cases} \qquad (2.20)$$

is a continuous pressure distribution with continuous derivative, and is wave-less if $x_1 = -3\pi, -5\pi, \ldots$. Figure 2.5 shows results at $x_1 = -3\pi$.

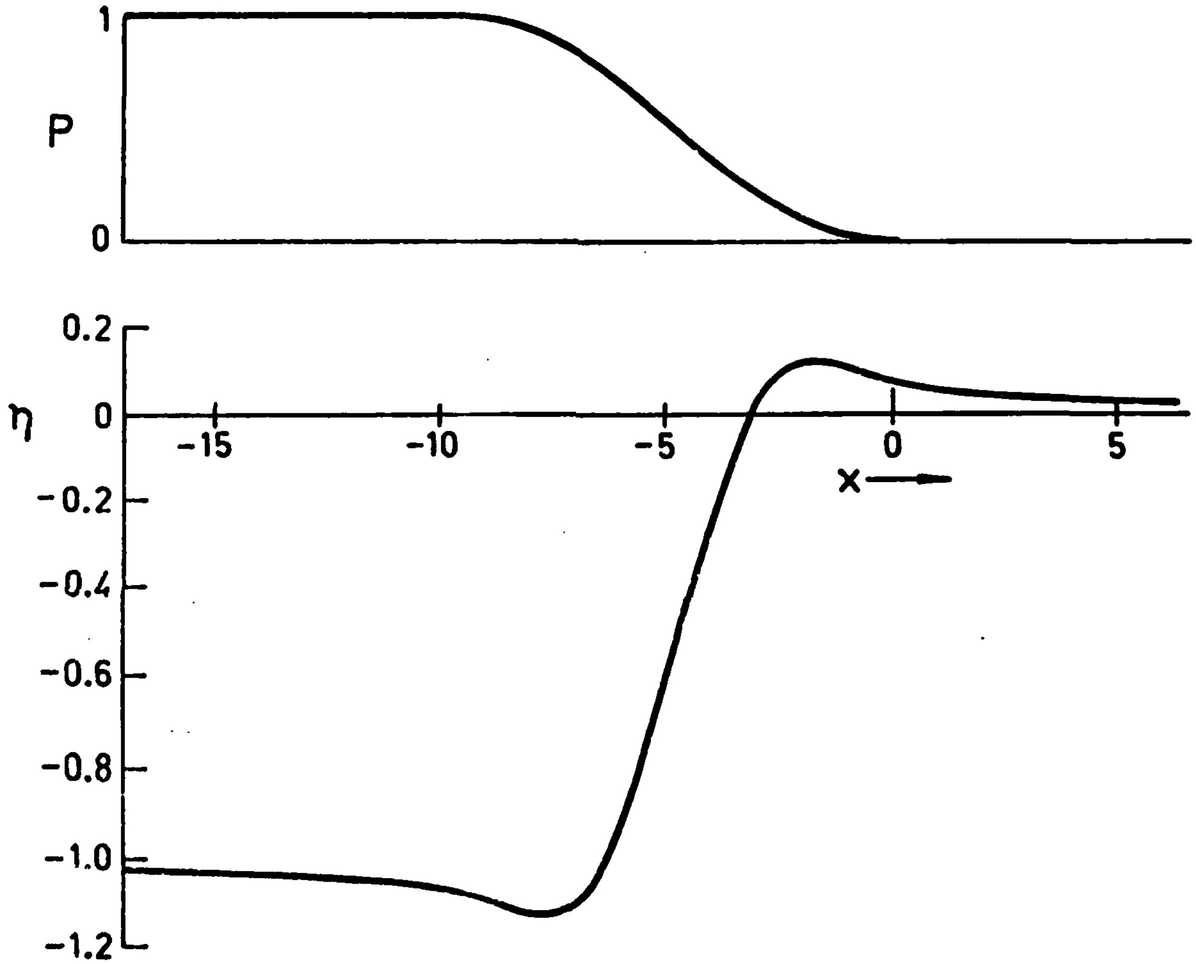

Fig. 2.5

Linearized free surface $\eta(x)$ generated by a wave-less pressure $P(x)$ that is continuous and has continuous first derivative, varying sinusoidally on the interval $-3\pi < x < 0$.

3. *Some properties and interpretations.*

The linearised free-surface flow produced by a wave-less pressure distribution has some interesting special properties. In particular, *symmetrical* wave-less pressures produce *symmetrical* flows, in the following sense. Suppose $x = x_s$ is a point of symmetry of a wave-less pressure $P(x)$, such that

$$P(x_s + X) = P(x_s - X) \qquad (3.1)$$

for all X. Then $x = x_s$ is also a point of symmetry of the free-surface elevation $\eta(x)$ produced by this pressure, i.e.

$$\eta(x_s + X) = \eta(x_s - X) \qquad (3.2)$$

Figure 2.2 illustrates this property, with $x_s = -\pi$ as the point of symmetry.

A similar result applies to what we might call "anti-symmetric" wave-less pressure distributions, but is most directly expressed in terms of derivatives. That is, if $x = x_s$ is a point of symmetry of the pressure *gradient*, such that

$$P'(x_s + X) = P'(x_s - X) \qquad (3.3)$$

for all X, then it is also a point of symmetry of the free-surface *slope*, i.e.

$$\eta'(x_s + X) = \eta'(x_s - X) \quad , \qquad (3.4)$$

Upon integration, we can re-phrase this anti-symmetry property to state that

$$P(x_s + X) - P(x_s) = P(x_s) - P(x_s - X) \qquad (3.5)$$

implies that

$$\eta(x_s + X) - \eta(x_s) = \eta(x_s) - \eta(x_s - X) \qquad (3.6)$$

Figures 2.1, 2.3, 2.4 and 2.5 all illustrate this property, for various values of x_s.

It is important to emphasize that these properties hold *only* for wave-less pressure distributions. It is obvious that solutions with waves cannot obey such symmetry conditions, since the radiation condition demands that the waves occur only at $x = +\infty$, and not at $x = -\infty$. The symmetry results can be proved by noting that $K(x)$ in (2.2) can be split into even and odd parts, but that the even part ($\cos x - 1/2$) contributes at most a constant to η, for wave-less pressures $P(x)$. On the other hand, the odd part of $K(x)$ nessarily generates (for *any* $P(x)$) solutions $\eta(x)$ satisfying the symmetry conditions.

Another almost self-evident property of wave-less pressures is that they are *reversible*. That is, if $P(x)$ generates $\eta(x)$, then $P(-x)$ generates $\eta(-x)$. In effect, we have simply reversed the direction of the free stream at infinity, and, with it, the whole flow.

Again, this property can be proved formally for the linearised solution by separating $K(x)$ into even and odd parts.

It is obviously *false* for wave-generating pressures, since the waves due to $P(x)$ must lie downstream, which means that those due to $P(-x)$ would lie upstream if reversibility held. In fact, this reversibility property holds not only for *weak* pressures $P(x)$ for which linearisation is justified, but also in the fully-non-linear case.

Once a flow due to a given pressure distribution $P(x)$ has been computed, it may be re-interpreted as that produced in the presence of a certain body. That is, the computed curve $y = \eta(x)$ is a streamline, and part or all of it may be replaced by a fixed impermeable boundary. In particular, suppose $P(x) = 0$ for $x < x_L$ and for $x > x_R$, but $P(x) \neq 0$ for $x_L < x < x_R$. Then the flow generated by this $P(x)$ is the same as that past a body with the equation $y = \eta(x)$, $x_L < x < x_R$, with a free surface at atmospheric pressure in $x < x_L$ and $x > x_R$. This interpretation holds whether or not the pressure $P(x)$ is wave-less.

In this way we can provide an *inverse* solution to problems involving ship-like bodies. Examples such as that in Fig. 2.2 where $P(x)$ is non-zero only over a finite segment appear at first glance to be the most relevant. However, pressures $P(x)$ that are non-zero on a semi-infinite segment, such as that used for Fig.2.1, generate flows that can be interpreted directly as those near the *stern* of a ship. In general, such stern flows generate downstream waves. However, in the special case where $P(x)$ is wave-less, the above reversibility property applies, and allows an additional interpretation as a flow near the *bow* of a ship.

Of course, no guarantee is available that the "body" shapes $y = \eta(x)$ so generated will be particularly ship-like, and *finite-length* bodies, like that of Fig. 2.2 tend to be very far from ship-like. On the other hand, the semi-infinite body shown in (for example) Fig. 2.5 is not unlike a bulbous bow, and the inverse technique appears to be quite promising if confined to local flow properties at the bow or stern.

In making this inverse interpretation of the linearised results of Section 2, we must not forget that these are approximations, and are formally only valid when $P(x)$ is so weak that the free-surface slope $\eta'(x)$ is everywhere small. If $y = \eta(x)$ is now interpreted as the surface equation of a ship-like body, this places severe restrictions on the applicability of the results. Fortunately, the inverse interpretation is not restricted to linearised solutions, and we now turn our attention to the full non-linear problem, whose solutions allow finite $\eta'(x)$, and hence finite slopes in the inversely-generated body surface.

4. *Less-Weak Pressures.*

If ϵ is a measure of the size of the pressure $P(x)$, then the results of Section 2 apply in the limit as $\epsilon \to 0$, and provide (ϵ) estimates of the free-surface shape, i.e. neglect all terms of $O(\epsilon^2)$ and smaller. It is now natural to seek an expansion in powers of ϵ, commencing with the $O(\epsilon)$ terms already worked out.

However, for a number of reasons, it is inconvenient (sometimes impossible) to carry out this analysis for a pressure P that is given as a function of the space variable x. Indeed, if the pressure is large enough, there may exist no such single-valued functional representation, since there may be more than one point on the free surface corresponding to a given value of x. It is preferable to represent the pressure P as a function of a variable that changes in a strictly monotone-increasing manner along the free surface.

Such a variable is the velocity potential ϕ. That is, we now suppose that the free-surface pressure $P(\phi)$ is a given function of ϕ. In the present non-dimensionalization, the undisturbed stream corresponds to $\phi = x$, so that this representation is identical, with $P(\phi) \equiv P(x)$, to that used in Section 2, to the order of approximation being used in that section. All results of Section 2 can now be carried over, with x replaced by ϕ.

We now consider $O(\epsilon^2)$ and higher perturbations. At the same time, it is convenient to suppose that the pressure P

itself can be modified as we expand to such higher orders. Thus we write

$$P(\phi) = \epsilon P_1(\phi) + \epsilon^2 P_2(\phi) + \epsilon^3 P_3(\phi) + \ldots \qquad (4.1)$$

Since ϵ was scaled to unity in Section 2, in fact the results of that section correspond to $P_1(\phi) \equiv P(x)$.

If $z = x+iy$, and $f = \phi + i\psi$ is the complex velocity potential, then we consider $z = z(f)$ and expand

$$z(f) = f + \epsilon z_1(f) + \epsilon^2 z_2(f) + \epsilon^3 z_3(f) + \ldots \qquad (4.2)$$

The free surface corresponds to $\psi = 0$, and the (scaled) dynamic free-surface condition is (with $g = 1$, $U = 1$, $\rho = 1$)

$$P + |z'(f)|^{-2}/2 + y = 1/2 \qquad (4.3)$$

Upon substitution of (4.1) and (4.2) and collecting powers of ϵ, we find that for all $j=1,2,3\ldots\ldots$

$$p_j + P_j - x_j' + y_j = 0 \qquad (4.4)$$

where all quantities are evaluated on $\psi = 0$, the prime denotes $\partial/\partial\phi$, and

$$p_1 = 0 \qquad (4.5)$$

$$p_2 = \frac{3}{2}x_1'^2 - \frac{1}{2}y_1'^2 \qquad (4.6)$$

$$p_3 = 3x_1'x_2' - y_1'y_2' + 2x_1'y_1'^2 - 2x_1'^3 \qquad (4.7)$$

$$p_4 = 3x_1'x_3' - y_1'y_3' + \frac{3}{2}x_2'^2 - \frac{1}{2}y_2'^2$$

$$- 6x_1'^2 x_2' + 4x_1' y_1' y_2' + 2x_2' y_1'^2 - 5x_1'^2 y_1'^2$$
$$+ \frac{5}{2}x_1'^4 + \frac{1}{2}y_1'^4 \qquad (4.8)$$

etc. Thus, at all orders of approximation j, we have the same type of boundary condition (4.4) the only complication at higher order being the manner in which the "equivalent linear" pressure P_j is determined from earlier terms in the expansion.

For $j = 1$, (4.4) and (4.5) are equivalent to the usual linearized free-surface boundary condition, and all results of Section 2 are available to yield solutions of this problem. Note that in the present notation,

$$y_1(\phi) = \eta(\phi) \qquad (4.9)$$

In fact, we need no more information from Section 2 than $\eta(x)$ (with x replaced by ϕ), since (4.4) and (4.9) imply

$$x_1'(\phi) = P_1(\phi) + \eta(\phi) \qquad (4.10)$$

If we turn to the 2nd-order terms $j = 2$, it is immediately apparent that step-function discontinuities in the input $P_1(\phi)$ are unacceptable, since they lead to (c.f.(2.13)) logarithmically-infinite free-surface slope,and via (4.6) to "log squared" singularities in the 2nd-order pressure p_2, and hence to an unbounded 2nd-order free-surface displacement y_2. This problem compounds itself at higher order, and one must suspect that no solution exists if $P(\phi)$ possesses a step discontinuity.

This is also a conclusion one is drawn to by direct consideration of the non-linear boundary condition (4.3), irrespective of any form of asymptotic expansion such as (4.2), and appears to be in conflict with the fact that Schwartz [7] claims to have found a non-linear numerical solution for such a pressure distribution. However, it is probable that Schwartz's numerical solution is not sufficiently accurate near the singular points to display this difficulty.

In any case, we choose to require that $P_1(\phi)$ be a *continuous* function, typically (2.18), (2.19) etc. For example, if P_1 is continuous but its derivative P_1' possesses a step-function discontinuity, then $y_1' = \eta_1'$ is bounded and continuous, and hence so is the second-order pressure p_2. We therefore expect no trouble at any order of approximation, and by implication, expect that the full non-linear problem does have a solution.

The symmetry properties of the linear wave-less solutions as discussed in Section 3, now play an important role in the non-linear theory. Suppose for example that $P_1(\phi)$ is wave-less and symmetric about some point $\phi = \phi_S$. Then, as we have seen, so is $\eta(\phi) = y_1(\phi)$, and thus so is $x_1'(\phi)$. Hence $p_2 - P_2$ is symmetric, and a symmetric second-order solution exists if the second-order input P_2 is taken as symmetric. A similar conclusion applies at all higher orders, and we may therefore expect to generate a fully non-linear symmetric solution. Note that in such a case P_2 is not arbitrary and cannot be set to zero; it is needed in order to cancel the waves at second order.

The case of "anti-symmetric" pressures is somewhat more interesting. Now if the pressure *gradient* P_1' is symmetric, then so is the free-surface slope $\eta' = y_1'$. Thus (3.6) implies that $p_2 - P_2$ is *symmetric*, and we can (indeed must) use a symmetric 2nd-order input P_2. Thus, at 2nd-order, the anti-symmetry property of the input pressure is necessarily destroyed, and it appears that there exists no wave-less non-linear anti-symmetric pressure distribution.

For example, suppose

$$P_1(\phi) = \begin{cases} 1, & -\infty < \phi < -2\pi \\ -\phi/2\pi, & -2\pi < \phi < 0 \\ 0, & \phi > 0 \end{cases} \tag{4.11}$$

This is just the "ramp" pressure of (2.18), expressed in terms of ϕ instead of x, and evaluated in the wave-less case $x_1 = -2\pi$. Note that this pressure is anti-symmetric about $\phi = -\pi$. This pressure can be used to compute $x_1(\phi)$ and $y_1(\phi)$, the latter being as plotted for $\eta(x)$ in Figure 2.4. Then we can easily compute $p_2(\phi)$ from (4.6), and this is given in Figure 4.1, which verifies that $P_2(\phi)$ is symmetric about $\phi = -\pi$. The complete second-order problem now has been reduced to a linear problem, in which the free surface is disturbed by a combination of the *input* second-order pressure $P_2(\phi)$, (which may or may not be present) and the computed pressure $p_2(\phi)$ as displayed in Figure 4.1, which must always be present.

If there is no input second-order pressure, i.e. if the pressure is given by a simple ramp to at least $O(\epsilon^3)$ accuracy, then waves *must* be generated. That is, by itself, the pressure $p_2(\phi)$ of Figure 4.1 *does* generate waves. If we demand a

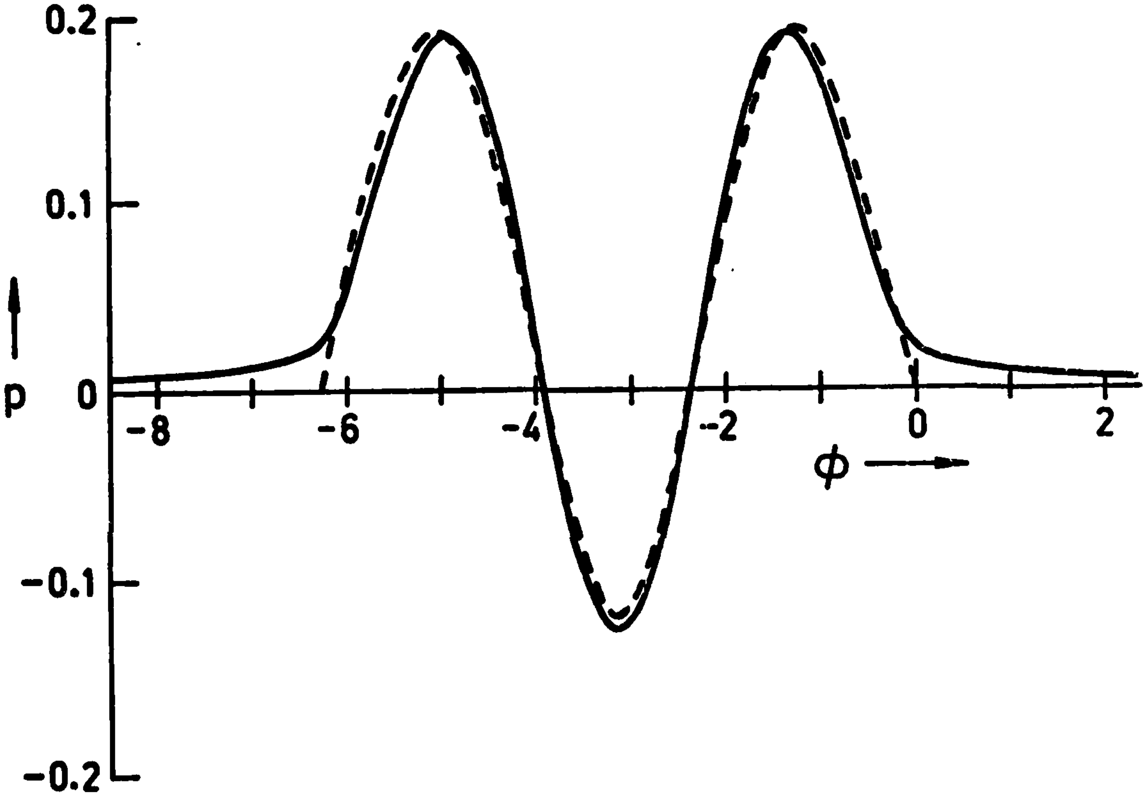

Fig. 4.1

The solid curve is the second-order pressure $p_2(\phi)$ corresponding to an input first-order pressure equivalent to the linear ramp of Fig. 2.4. The dashed curve is a wave-less analytic approximation to the solid curve for $-2\pi < \phi < 0$, given by equation (4.15).

wave-less solution at second order, we must incorporate some input pressure $P_2(\phi)$ at second order, of such a nature and magnitude as to cancel the waves generated by $p_2(\phi)$. The symmetry principle demands that this input pressure must be symmetric about $\phi = -\pi$, and there are many choices for $P_2(\phi)$ that are satifactory.

A rather attractive possibility is to choose

$$P_2(\phi) = -p_2(\phi) \tag{4.12}$$

in which case there is no pressure distribution *at all* at 2nd-order, and hence no second-order flow. That is, without further ado, we can assert that an input pressure

$$P(\phi) = \epsilon P_1(\phi) - \epsilon^2 p_2(\phi) \tag{4.13}$$

where $P_1(\phi)$ is given by (4.11) and $p_2(\phi)$ by Figure 4.1 produces a wave-less flow field.

$$z = \epsilon z_1(f) + O(\epsilon^3) \tag{4.14}$$

One difficulty of the assumption (4.12) is that since $p_2(\phi) \neq 0$ in $\phi > 0$, the same applies to $P_2(\phi)$. That is, there is no true free surface on which $p = 0$, the input pressure being non-zero everywhere.

Alternatively, a good choice for $P_2(\phi)$ is one that, while remaining zero for $\phi > 0$ and generating *exactly* equal and opposite waves to p_2, also cancels $p_2(\phi)$ for $-2\pi < \phi < 0$, to as great an extent as possible. One such choice, found by trial and error, is

$$-P_2(\phi) = \begin{cases} -\,0.118 \sin 3\phi/2 + 0.09 \sin^2\phi, & -2\pi < \phi < 0. \\ 0 \hspace{6em}, & \text{otherwise} \end{cases} \tag{4.15}$$

which is shown (dashed) in Figure 4.1. Note that the first term of (4.15) generates the waves to cancel those of p_2; the second term is itself wave-less, and the coefficient 0.09 is simply chosen to match $-P_2$ to p_2 as closely as possible. It is now quite straight-forward to compute the free-surface elevation y_2 produced by the everywhere-small residual pressure P_2+p_2, and this is shown in Figure 4.2. Note the small absolute size of y_2, which suggests that these results may retain validity up to quite large values of ϵ.

The actual free-surface shape in physical-space coordinates (x,y), is given by

$$\begin{aligned} x &= \phi + \epsilon x_1(\phi) + O(\epsilon^2) \\ y &= \epsilon y_1(\phi) + \epsilon^2 y_2(\phi) + O(\epsilon^3). \end{aligned} \tag{4.16}$$

To obtain a result for $y = y(x)$, consistently with error $O(\epsilon^3)$, we can treat (4.16) as a pair of parametric equations, with ϕ as a parameter. The small magnitude of $y_2(\phi)$ in the example of Figure 4.2 means that (for moderate ϵ), the y-coordinate of the free surface is little changed by second-order effects in this example. However, the $O(\epsilon)$ correction to the x-coordinate is not so small, and represents the most significant non-linear modification. We return to this question in the following section.

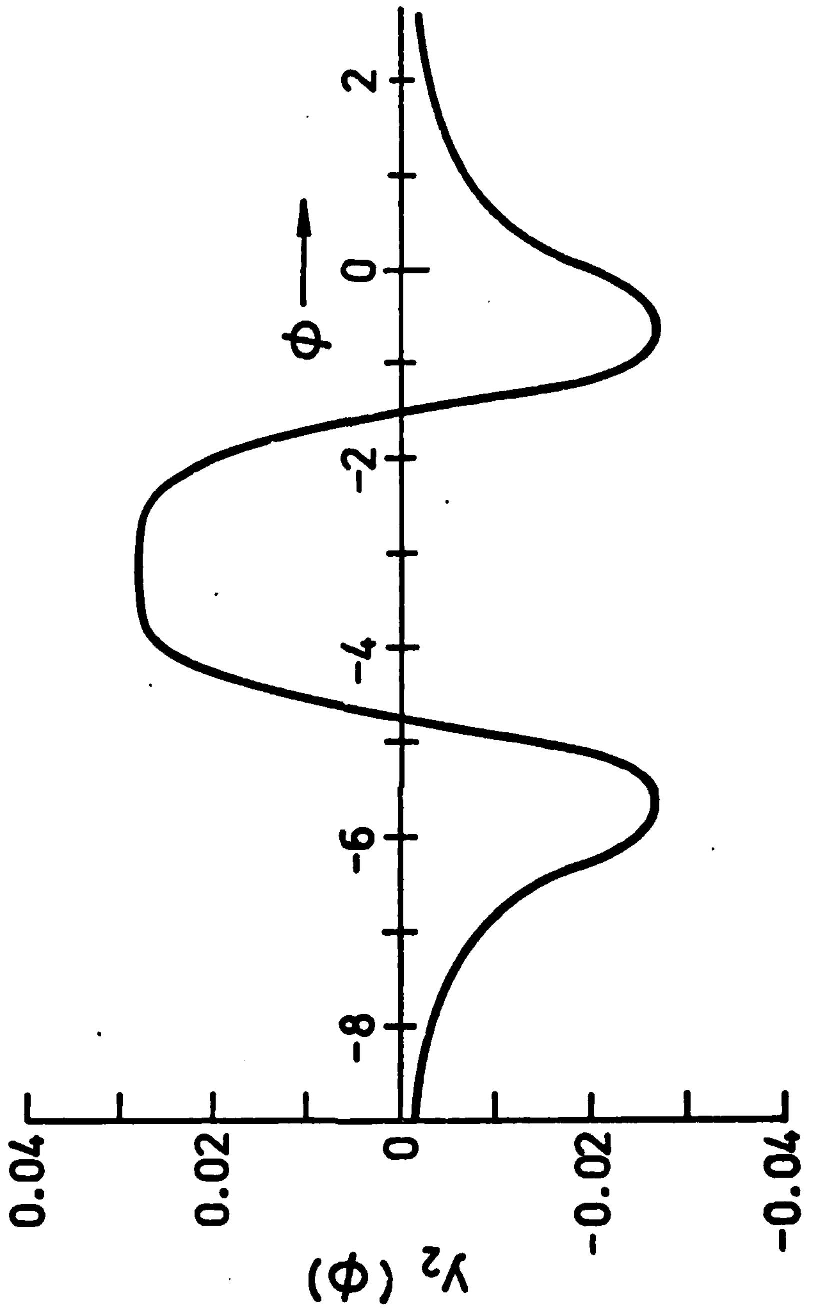

Fig. 4.2

The second-order contribution to the free-surface elevation, for the case when the first-order input pressure is the linear ramp of Fig. 2.4, and the second-order input pressure is as given by the dashed curve of Fig. 4.1, i.e. by equation (4.15).

5. *Strong Pressures*

An exact inverse method of solution of the present class of problem is always available. That is, given any function $z(f)$ that is analytic in the lower half f-plane, we can use (3.3) directly to compute the free-surface pressure $P(\phi)$. One way to do this is to combine a uniform stream with singularities *above* the free surface.

For example, suppose

$$z(f) = f + 12\log(f-4i) + \frac{48+64i}{f+4-12i} \qquad (5.1)$$

If linearisation (i.e. $f \approx z$) were legitimate, (5.1) could be interpreted as a stream plus a *sink* at (0,4) and a *dipole* at (-4,12). However, the size of the coefficients in (5.1) makes linearisation of doubtful value, even for qualitative purposes. Figure 5.1 shows the streamline $x+iy = z(\phi+i0)$ computed from (5.1). Since we have scaled $g = U = 1$, and the "draft" of the shape shown in Figure 5.1 is 12π, the draft-based Froude number for this flow is $(12\pi)^{-1/2} = .163$. The shape shown is quite like a typical bow.

The pressure P (obtainable from (3.3)) is almost hydrostatic, and is significant only for $y < 0$. Indeed, if $y > 0$, then $P/P_1 < .008$, where P_1 is the pressure at $x = -\infty$. The coefficients and singularity locations were in fact chosen by trial and error so that this would be so. Many other choices of the parameters in (5.1) led to a similar property, and shapes having small pressure for sufficiently large ϕ or x can be constructed at any draft-based Froude number. However,

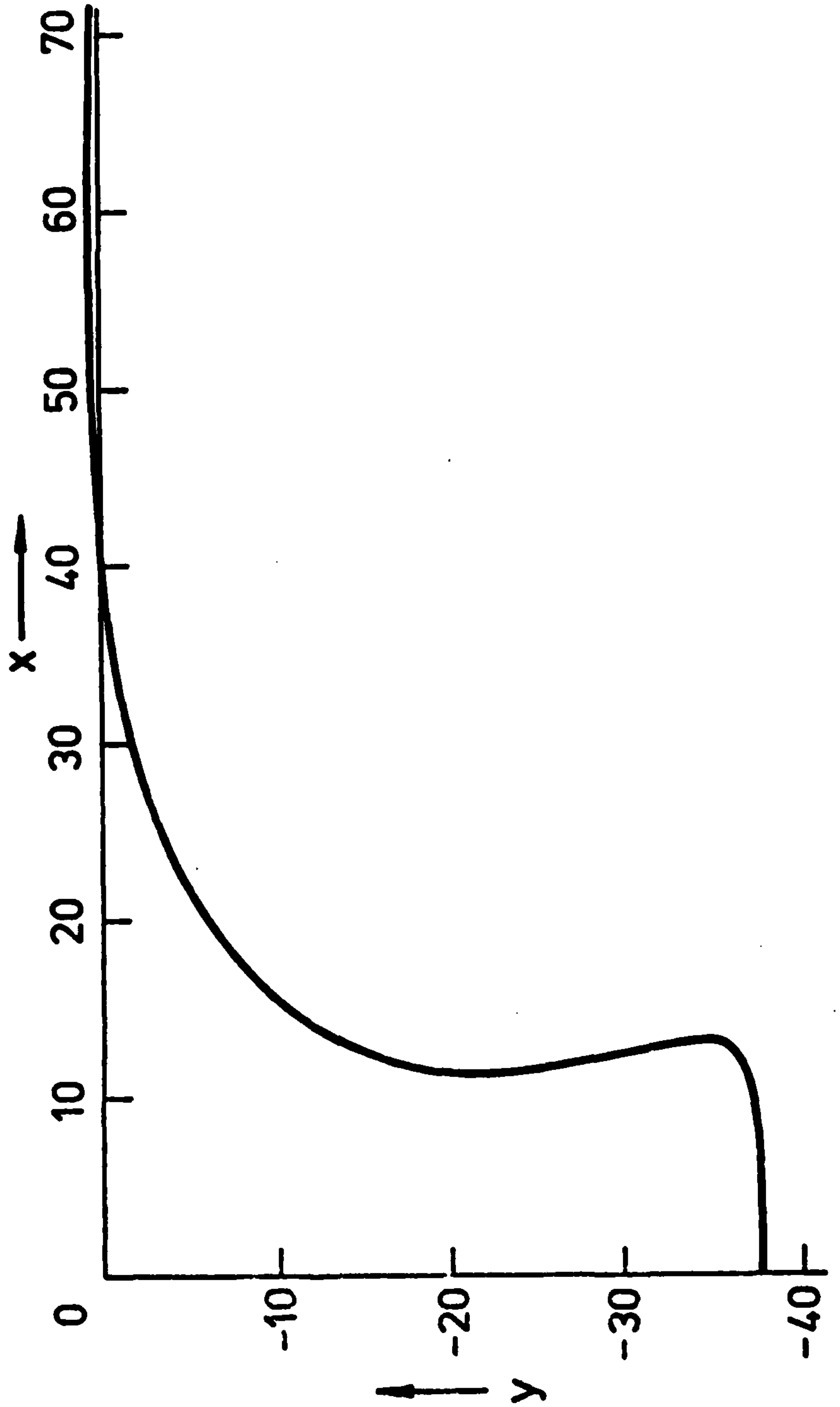

Fig. S.1

The streamline $\psi = 0$ of the flow defined by equation (S.1).

this procedure seems hard to carry through in any systematic manner, and we turn to an alternative procedure based on the linearized solution.

Flows satisfying the exact free-surface condition (3.3) can be constructed in a systematic manner by making use of the results already obtained in the previous sections. For example, suppose we set

$$z = f + \epsilon z_1(f) \tag{5.2}$$

(*exactly*), where $z_1(f)$ is the linear solution corresponding to some input "seed" pressure $P_1(\phi)$. Then the flow (5.2) can be considered to have been generated by the free-surface pressure $P(\phi)$ given *exactly* by

$$P(\phi) = \frac{1}{2} - \epsilon y_1(\phi) - \frac{1}{2}\left[(1 + \epsilon x_1'(\phi))^2 + (\epsilon y_1'(\phi))^2\right]^{-1} \tag{5.3}$$

Note that in order to generate the free-surface shape and pressure P, we need only compute the linearised free-surface elevation $\eta(x)$ with $\epsilon=1$, since then $y_1(\phi) = \eta(\phi)$, and $x_1'(\phi) = P_1(\phi)+\eta(\phi)$. We can then compute very rapidly a complete family of exact non-linear solutions, by varying the amplitude parameter ϵ. The free-surface shape is given parametrically by

$$x = \phi + \epsilon\int_{-\infty}^{\phi}[P_1(\phi)+\eta(\phi)]\, d\phi$$

$$y = \epsilon\eta(\phi) \tag{5.4}$$

As ϵ varies, the y-coordinate simply scales in proportion, but the actual shape of the free-surface distorts, because of the non-proportional dependence of x on ϵ.

Figure 5.2 shows free-surface shapes computed in this way for various values of ϵ, with the seed pressure $P_1(\phi)$ given by the simple ramp (4.11). These curves are drawn true to scale, and their non-linearity is confined by the large slopes. However, the curve shown for $\epsilon = 1$ does not display large slopes, and hence it is almost the same as Figure 2.4, since linearization is not too much in error. As ϵ increases, the "downward bulb" at $\phi = -5.5$ becomes sharper, whereas the "upwrd bulb" at $\phi = -1$ (which is in Figure 2.4 exactly a reversed image of the downward bulb) is smoothed out.

Eventually, at about $\epsilon = 3.1$, the downward bulb sharpens into a cusp, and for ϵ values greater than this, non-physical looped shapes are generated. The distorted variation in the x-coordinate now allows a non-single-valued $y = y(x)$ free surface, containing a point where the free surface is vertical, and this actually happens for ϵ values near to 3 in this example.

For each separate value of ϵ, we must compute the actual free-surface pressure $P(\phi)$ by (5.3). Thus every curve shown in Figure 5.2 corresponds to a different $P(\phi)$. As the downward bulb becomes sharper, the fluid velocity increases near the corner, and hence the pressure $P(\phi)$ decreases, until at the value of ϵ where the body is cusped, $P \to -\infty$ at the cusp. Figure 5.3 (solid curves) repeats the free-surface shape of Fig. 5.2 at $\epsilon = 2$, and shows the corresponding pressure P, plotted as a function of x.

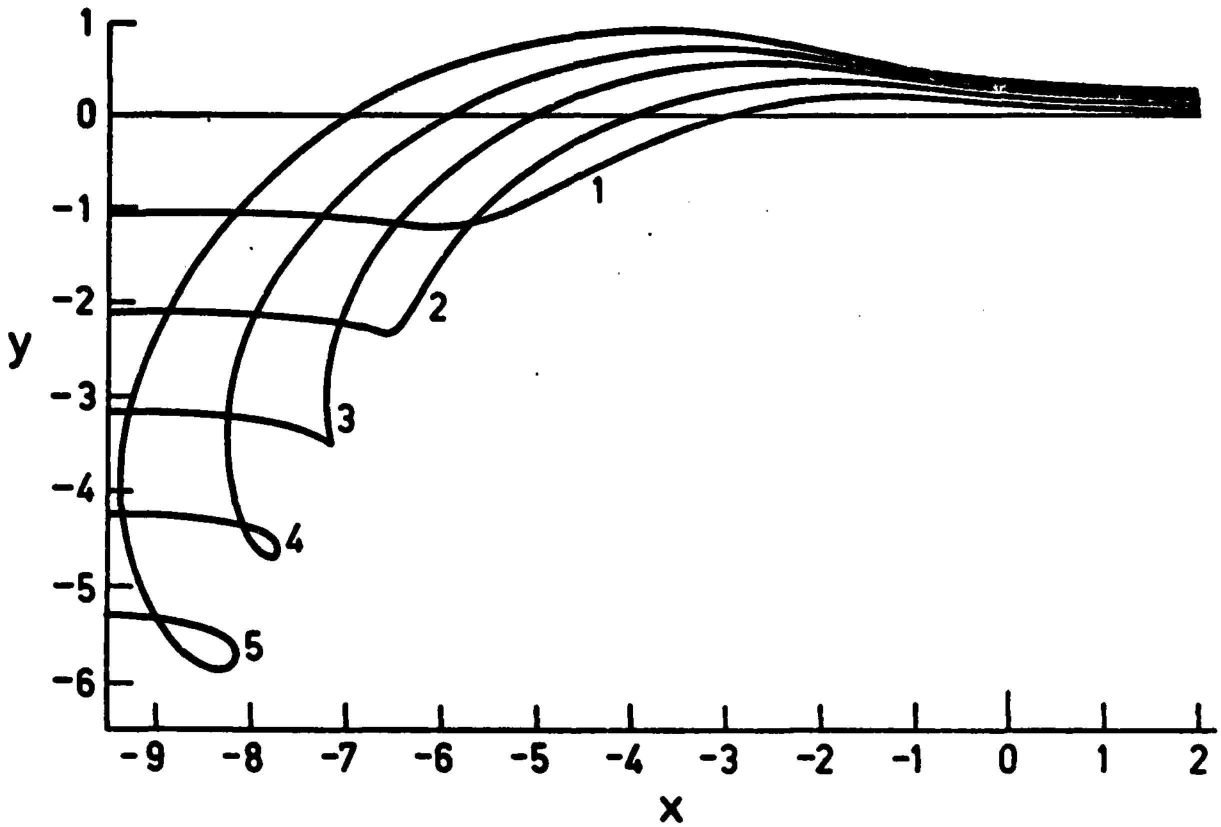

Fig. 5.2

A set of exact non-linear streamlines $\psi = 0$ for flows seeded by the linear ramp pressure of Fig. 2.4, for various values of a parameter ϵ measuring the magnitude of the input pressure.

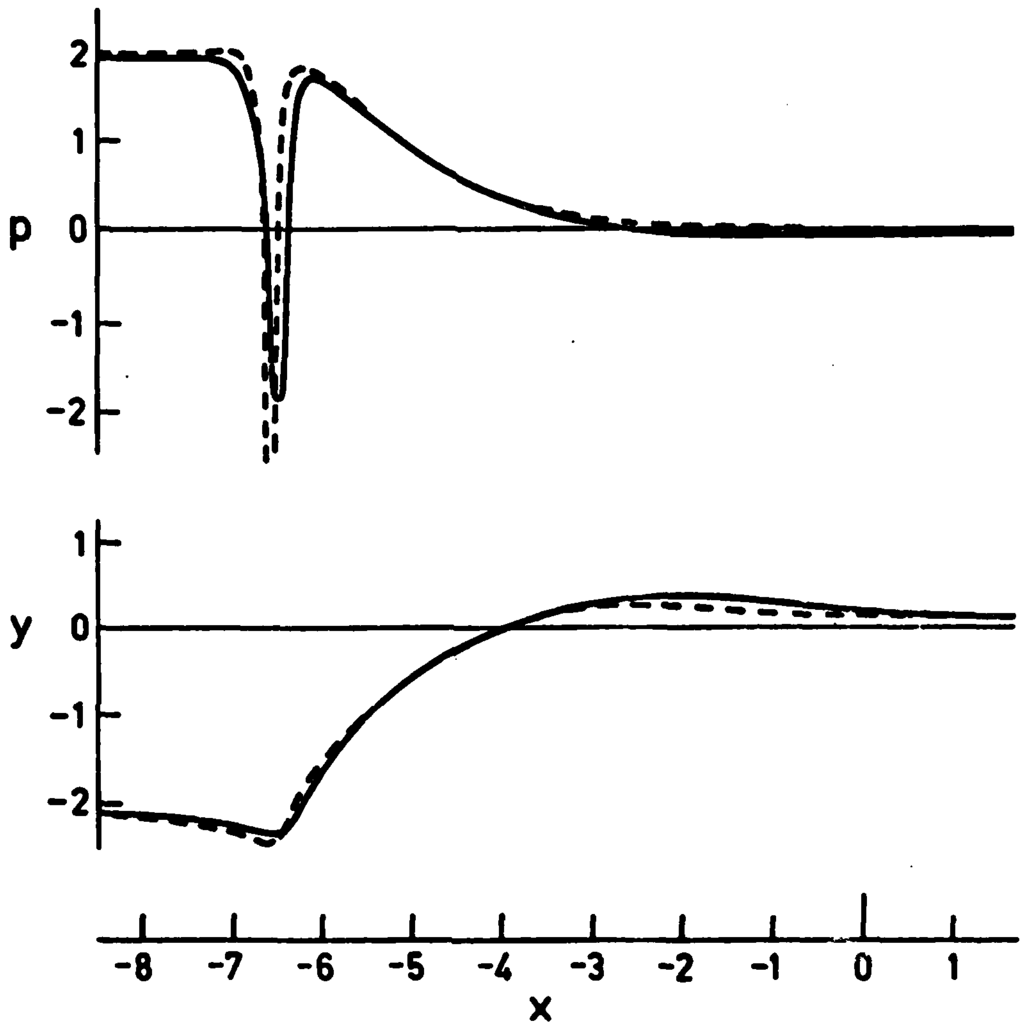

Fig. 5.3

The solid curves show the output pressure and (repeated) streamline shape for the curve $\epsilon = 2$ of Fig. 5.2. The dashed curve corresponds to a similar computation, but with both first- and second-order seed pressures, the latter being as in Fig. 4.1.

In fact it is interesting to note that the present exact procedure generates almost the same results as the 2nd-order procedure (4.16). The only difference between (4.16) and (5.4) is the term $\epsilon^2 y_2(\phi)$ in the former, and we have indicated in Section 4 that this term can be made quite small. That is, the second-order accurate free surface computed at $\epsilon = 2$ using (4.16), with P_1 given by (4.11) and P_2 by (4.15), is almost indistinguishable from that shown in Figure 5.3. However, the pressure $P(\phi) = \epsilon P_1 + \epsilon^2 P_2$ now vanishes *exactly* for all $\phi > 0$, so that there is a true free-surface present.

The present exact inverse method can be extended to take account of both 1st and 2nd-order seed pressure. That is, suppose instead of (5.2) we set

$$z = f + \epsilon z_1(f) + \epsilon^2 z_2(f) \tag{5.5}$$

where $z_1(f)$ and $z_2(f)$ are 1st and 2nd-order solutions generated by $P_1(\phi)$ and $P_2(\phi)$ respectively. Then this is also the *exact* solution generated by the pressure

$$P(\phi) = \frac{1}{2} - \epsilon y_1(\phi) - \epsilon^2 y_2(\phi) - \frac{1}{2}[(1+\epsilon x_1'(\phi)+\epsilon^2 x_2'(\phi))^2 + (\epsilon y_1'(\phi)+\epsilon^2 y_2'(\phi))^2]^{-1} \tag{5.6}$$

Figure 5.3 also shows (dashed) computations using (5.5), (5.6), for $\epsilon = 2$, with P_1 given by (4.11) and P_2 by (4.15). The dashed and solid curves are generally close, although the dashed downward bulb is significantly sharper, and hence the pressure minimum is stronger.

However, the most important change is not easy to see on the scale of the figure, and this is the fact that there is a range ($x > -1.4$) over which the pressure P computed from (5.6), satisfies $|P| < 0.01$. In the same range $x > -1.4$, the solid curve still has only $|P| < 0.06$. That is, this portion of the dashed streamline is much more nearly "free" than the solid one. Clearly one could continue this process to even higher orders, generating each time an exact solution, with the property that, as the order of the process increases, $P \to 0$ for $\phi > 0$.

6. *Conclusion*

We have demonstrated in this paper, both by linear and non-linear methods, some families of free-surface pressure distributions that do not generate waves. Since these wave-less flows can be reversed in direction, they also generate candidate shapes for splash-less bows.

References

1. Baba, E., "Wave-Breaking Resistance of Ships,", Proc. Int. Seminar on Wave Resistance, Tokyo, Soc. Nav. Arch. Japan, 1976.

2. Miyata, H., "Characteristics of Non-Linear Waves in the Near Field of Ships, and their Effects on Resistance," 13th Symp. Naval Hydro, Office of Naval Research, Washington D.C., 1980

3. Vanden Broeck, J.-M., Schwartz, L.W., and Tuck E.O., "Divergent Low-Froude Number Series Expansion of Non-Linear Free-Surface Problems," Proc. Roy. Soc. Lond., Ser.A., Vol 361, 1978, pp. 207-224.

4. Vanden Broeck, J.-M. and Tuck E.O., "Computation of Near-Bow or Stern Flows, using Series Expansion in the Froude Number," 2nd. Int. Conf. on Numerical Ship Hydro., Berkeley, 1977.

5. Shmidt, G.H., "Linearized Stern Flow of a Two-Dimensional Shallow-Draft Ship", J.Ship Res., Vol. 25, 1981, pp.236-242.

6. Lamb, H. *Hydrodynamics*, Cambridge and Dover, 1932.

7. Schwartz, L.W., "Non-Linear Solution for an Applied Over-Pressure on a Moving Stream," *J. Eng. Math.*, Vol. 15, 1981, pp.147-156.

8. Forbes, L.K. "Non-Linear Drag-Free Flow over a Submerged Semi-Ellip tical Body", *J. Eng. Math.*, Vol. 16, 1982, pp.171-180.

9. Tulin, M.P. "An Exact Theory of Gravity Wave Generation by Moving Bodies, its Approximation, and its Implications", 14th Symp. Nav. Hydro., Ann Arbor, 1982. Office of Naval Research.

10. Sautreaux, C., "Mouvement d'un Liquide Parfait Soumis a la Pesanteur. Determination des Lignes de Courant," *J. Math. Pure Appl.* (5), Vol. 7, 1901, pp.125-159.

11. Tuck E.O., "On Air Flow over Free Surfaces of Stationary Water," *J. Austral. Math. Soc.*, Ser. B, Vol. 19, 1975, pp.66-80.

12. Wehausen, J.V. and Laitone, E.V., "Surface Waves," in *Handb. der Physik*, Vol. 9, ed. Flugge, S., Springer-Verlag, Berlin, 1960.

13. Tuck, E.O., "Linearized Planing-Surface Theory with Surface Tension. Part I: Smooth Detachment", *J. Austral. Math. Soc.*, Ser. B., Vol. 23, 1982, pp. 241-258.

14. Abramowitz, M., and Stegun, I.A., *Handbook of Mathematical Functions*, Dover, New York, 1964.

SECURITY CLASSIFICATION OF THIS PAGE (When Data Entered)

REPORT DOCUMENTATION PAGE

READ INSTRUCTIONS BEFORE COMPLETING FORM

1. REPORT NUMBER: 2679	2. GOVT ACCESSION NO.: AD-A141 630
3. RECIPIENT'S CATALOG NUMBER	
4. TITLE (and Subtitle): WAVE-LESS FREE-SURFACE PRESSURE DISTRIBUTIONS	5. TYPE OF REPORT & PERIOD COVERED: Summary Report - no specific reporting period
	6. PERFORMING ORG. REPORT NUMBER
7. AUTHOR(s): J.-M. Vanden-Broeck and E. O. Tuck	8. CONTRACT OR GRANT NUMBER(s): DAAG29-80-C-0041 MCS800-1960
9. PERFORMING ORGANIZATION NAME AND ADDRESS: Mathematics Research Center, University of Wisconsin, 610 Walnut Street, Madison, Wisconsin 53706	10. PROGRAM ELEMENT, PROJECT, TASK AREA & WORK UNIT NUMBERS: Work Unit Number 2 - Physical Mathematics
11. CONTROLLING OFFICE NAME AND ADDRESS: (See Item 18 below)	12. REPORT DATE: April 1984
	13. NUMBER OF PAGES: 40
14. MONITORING AGENCY NAME & ADDRESS (if different from Controlling Office)	15. SECURITY CLASS. (of this report): UNCLASSIFIED
	15a. DECLASSIFICATION/DOWNGRADING SCHEDULE

16. DISTRIBUTION STATEMENT (of this Report)

Approved for public release; distribution unlimited.

17. DISTRIBUTION STATEMENT (of the abstract entered in Block 20, if different from Report)

18. SUPPLEMENTARY NOTES

U. S. Army Research Office
P. O. Box 12211
Research Triangle Park
North Carolina 27709

National Science Foundation
Washington, DC 20550

19. KEY WORDS (Continue on reverse side if necessary and identify by block number)

Bow flow, free surface flows

20. ABSTRACT (Continue on reverse side if necessary and identify by block number)

Linear and nonlinear studies are made of two-dimensional free-surface flows under gravity, in which a disturbance is caused to an otherwise-uniform stream by a distribution of pressure over the free surface. In general, such a disturbance creates a system of trailing waves. However, there are special disturbances that do not, and some categories of such disturbances are discussed here. This work has potential applications to design of splash-less ship bows.

END

FILMED

DTIC